The Role of Modeling in the Development of High Efficiency Silicon Solar Cells

Dick Swanson

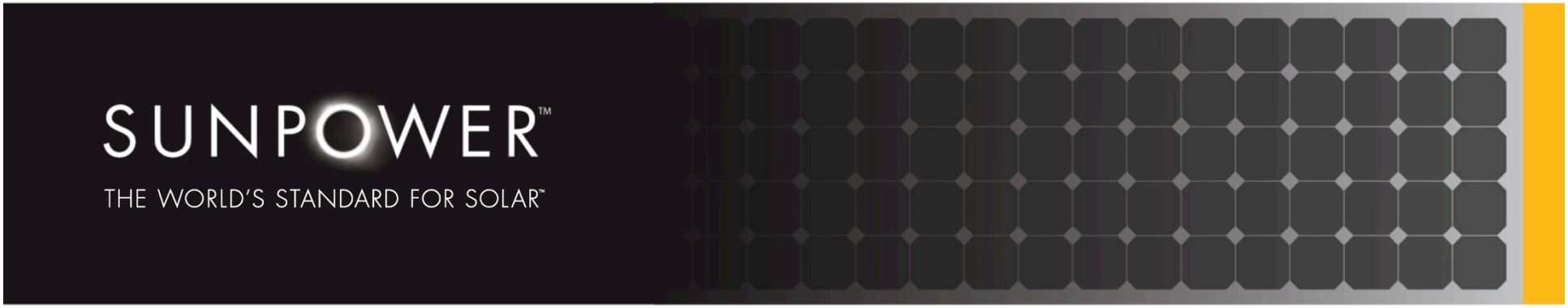

Presented at:

Challenges in PV Science, Technology, and Manufacturing:
A workshop on the role of theory, modeling, and simulation

Purdue University, August 2-3, 2012

1970s Solar Cell Analysis

Approach: Think of a solar cell as a big diode and
solve the semiconductor device modeling equations

Current = Drift + Diffusion
Continuity: dJ/dx = Volume Generation - Volume Recombination
Voltage = $kT/q \ln(nN_A/n_i^2)$ - Resistance Loss

Problem: Not Very Obvious How Cell Converts Light Energy
Into Electric Energy

- No explicit mention of total photo-generation
- Lots of approximations are involved
- Hard to grasp three dimensional effects

while at the junction edge, the excess carrier density is reduced to zero by the electric field in the depletion region

$$p_n - p_{n0} = 0 \qquad [x = x_j]. \tag{13}$$

Using these boundary conditions in (11), the hole density is found to be

$$(p_n - p_{n0}) = \left[\alpha F(1-R)\tau_p/(\alpha^2 L_p^2 - 1)\right] \left[\frac{\left(\frac{S_p L_p}{D_p} + \alpha L_p\right)\sinh\frac{x_j - x}{L_p} + \exp(-\alpha x_j)\left(\frac{S_p L_p}{D_p}\sinh\frac{x}{L_p} + \cosh\frac{x}{L_p}\right)}{\frac{S_p L_p}{D_p}\sinh\frac{x_j}{L_p} + \cosh\frac{x_j}{L_p}} - \exp(-\alpha x)\right] \tag{14}$$

and the resulting hole photocurrent density per unit bandwidth at the junction edge is

$$J_p = \left[\frac{qF(1-R)\alpha L_p}{(\alpha^2 L_p^2 - 1)}\right] \times \left[\frac{\left(\frac{S_p L_p}{D_p} + \alpha L_p\right) - \exp(-\alpha x_j)\left(\frac{S_p L_p}{D_p}\cosh\frac{x_j}{L_p} + \sinh\frac{x_j}{L_p}\right)}{\frac{S_p L_p}{D_p}\sinh\frac{x_j}{L_p} + \cosh\frac{x_j}{L_p}} - \alpha L_p \exp(-\alpha x_j)\right]. \tag{15}$$

This is the photocurrent that would be collected from the top side of a N/P junction solar cell at a given wavelength, assuming this region to be uniform in lifetime, mobility, and doping level.

To find the electron current collected from the base of the cell, (7) and (9) are used, making the same approximation as before that the base is uniform in its electrical properties. The boundary conditions are:

$$(n_p - n_{p0}) = 0 \qquad [x = x_j + W], \tag{16}$$

$$S_n(n_p - n_{p0}) = -D_n[d(n_p - n_{p0})/dx] \qquad [x = H], \tag{17}$$

where W is the width of the depletion region and H is the width of the entire cell. Equation (16) states that the excess minority carrier density is reduced to zero at the edge of the depletion region, while (17) states that surface recombination takes place at the back of the cell. (If the back is covered with an Ohmic contact, a perfect "sink" for the minority carriers exists and S_n can be taken as infinite.)

Using these boundary conditions, the electron distribution in a uniform p-type base is

$$(n_p - n_{p0}) = \frac{\alpha F(1-R)\tau_n}{(\alpha^2 L_n^2 - 1)}\exp[-\alpha(x_j + W)]\left[\cosh\frac{x - x_j - W}{L_n} - \exp[-\alpha(x - x_j - W)] - \frac{\left(\frac{S_n L_n}{D_n}\right)\left[\cosh\frac{H'}{L_n} - \exp(-\alpha H')\right] + \sinh\frac{H'}{L_n} + \alpha L_n \exp(-\alpha H')}{(S_n L_n/D_n)\sinh(H'/L_n) + \cosh(H'/L_n)}\sinh\frac{x - x_j - W}{L_n}\right] \tag{18}$$

and the photocurrent per unit bandwidth due to electrons collected at the junction edge is

$$J_n = \frac{qF(1-R)\alpha L_n}{(\alpha^2 L_n^2 - 1)}\exp[-\alpha(x_j + W)] \times \left[\alpha L_n - \frac{\frac{S_n L_n}{D_n}\left(\cosh\frac{H'}{L_n} - \exp(-\alpha H')\right) + \sinh\frac{H'}{L_n} + \alpha L_n \exp(-\alpha H')}{\frac{S_n L_n}{D_n}\sinh\frac{H'}{L_n} + \cosh\frac{H'}{L_n}}\right] \tag{19}$$

where H' is the total cell thickness minus the junction depth and depletion width, $H' = H - (x_j + W)$.

Some photocurrent collection takes place from the depletion region as well. The electric field in this region can be considered high enough that photogenerated carriers are accelerated out of the depletion region before they can recombine, so that the photocurrent per unit bandwidth is equal simply to the number of photons absorbed

New Method, 1980s.
View operation as an energy conversion process

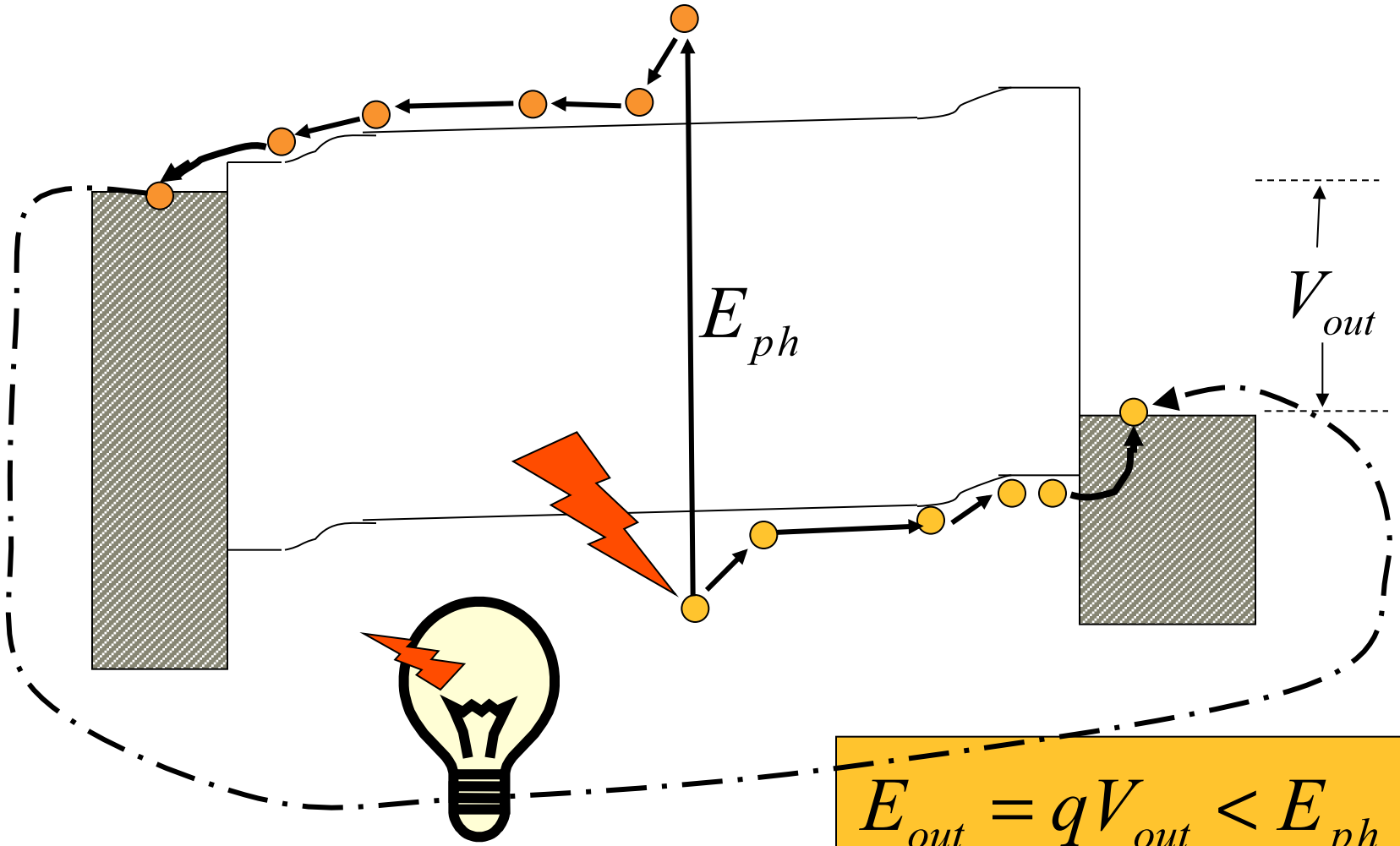

$$E_{out} = qV_{out} < E_{ph}$$

Cell Voltage

Difference in quasi-Fermi levels (or electrochemical potential)
At the positive and negative metal contacts

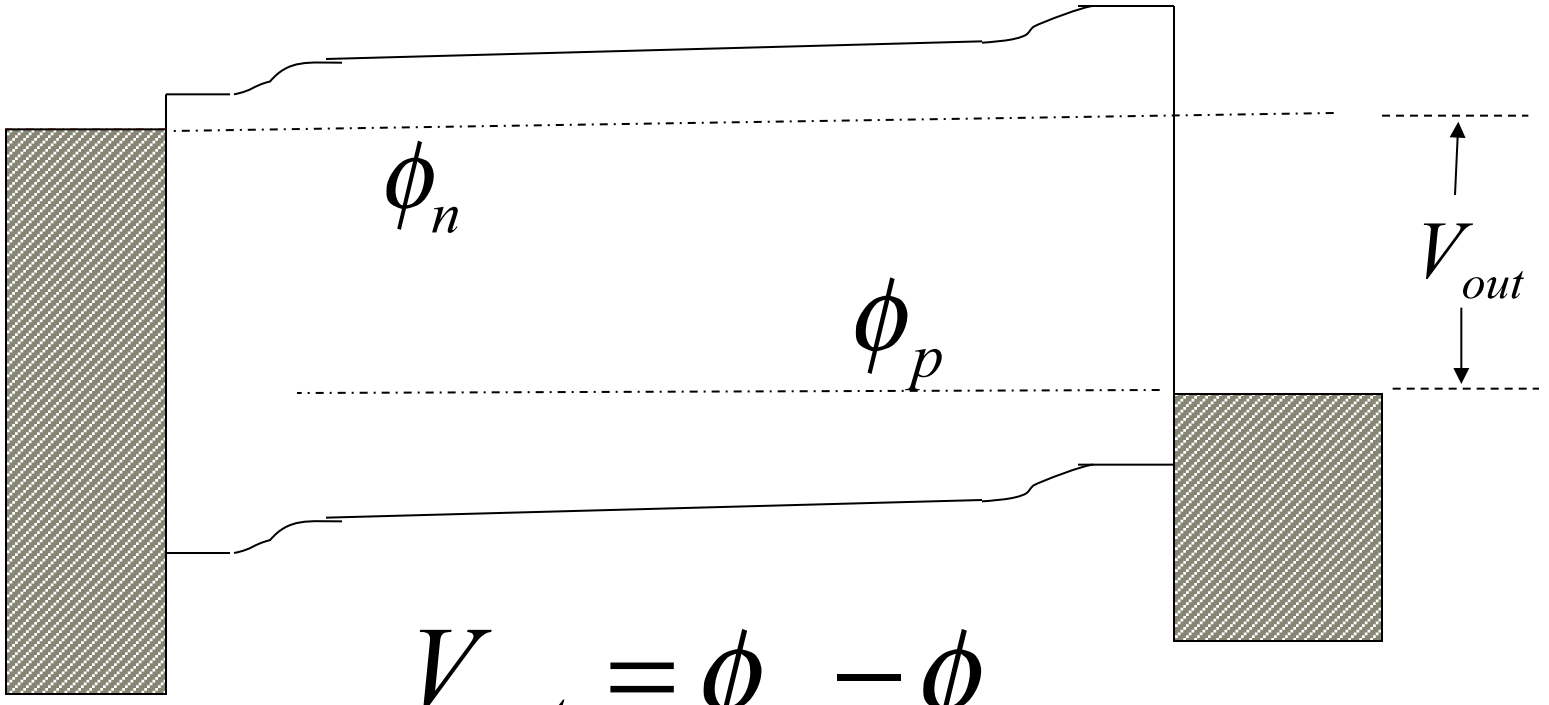

$$V_{out} = \phi_p - \phi_n$$

Integral forms of current are exact consequence of transport equations

$$I = I_{\mathrm{ph}} - I_{\mathrm{b,rec}} - I_{\mathrm{s,rec}} - I_{\mathrm{cont,rec}}$$

where

$$I_{\mathrm{ph}} = q \int_V g_{\mathrm{ph}} \, \mathrm{d}v$$ photoproduction current

$$I_{\mathrm{b,rec}} = q \int_V r \, \mathrm{d}v$$ bulk recombination

$$I_{\mathrm{s,rec}} = \int_S \vec{J}_{\mathrm{p}} \cdot \hat{n} \, \mathrm{d}S$$ surface recombination

$$I_{\mathrm{cont,rec}} = \int_{S_2} \vec{J}_{\mathrm{p}} \cdot \hat{n} \, \mathrm{d}S - \int_{S_1} \vec{J}_{\mathrm{n}} \cdot \hat{n} \, \mathrm{d}S$$ contact recombination

Cell Current

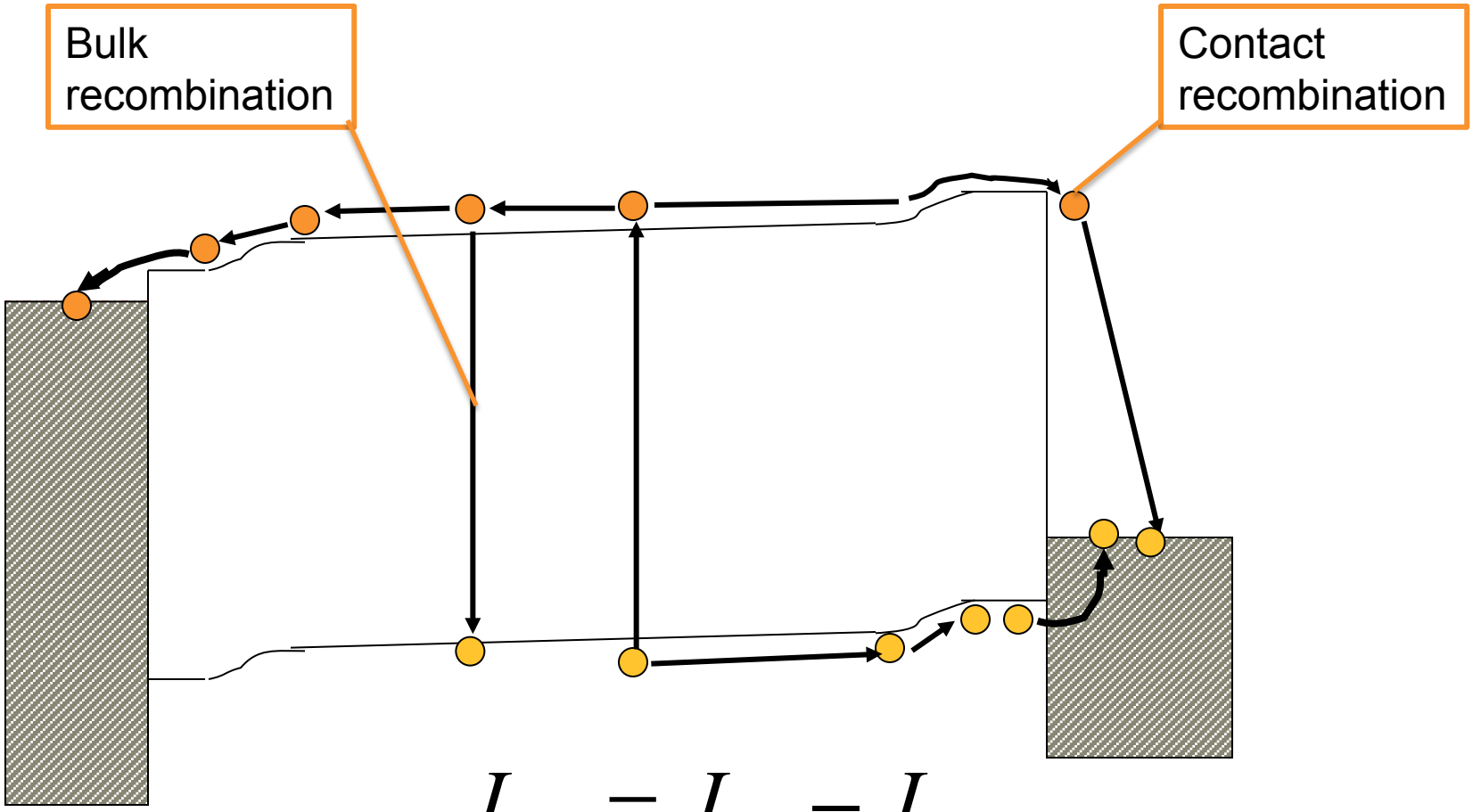

$$J_{out} = J_{ph} - J_{rec}$$

Dick Schwartz summed up the new view best:

Think of a bucket with leaks at different heights. Photons are like water pouring into the bucket raising the water level. The water level is like excess carrier density, or equivalently like increased separation of quasi-Fermi levels, or equivalently like increased difference in electron and hole electrochemical potential. The water rises until leaks balance inflow. If you plug one source of leakage (recombination), the level will rise until another is found. The object is to plug as many sources of recombination as possible.

Required Modeling Parameters

Parameter		Old (1975)
Intrinsic carrier conc.	n_i	1.45E10 cm-2
Ambipolar Auger coef.	C_a	3.8E-31 cm^6/s ($C_n + C_p$)
Minority carrier mobility	μ_n, μ_p	Same as majority carrier mobility
Ambipolar Diff. Coef	D_a	Decreases as mobiiity
Bandgap shrinkage	ΔE_g	All over the map
Absorption coef.	$\alpha(\lambda)$	Not known near band edge
Surface rec. veloicty	s	Poorly characterized
Radiative rec. coef.	B	2.1E-15 cm^3/s to 9.5E-15 cm^3/s
Specific contact res.	R_c	Poorly characterized
Light trapping		Not understood
2D and 3D effects		Not considered

All Parameters Changed with Close Inspection

Parameter		Old (1975)	New
Intrinsic carrier conc.	n_i	1.45E10 cm-2	1.01E10
Ambipolar Auger coef.	C_a	3.8E-31 cm^6/s ($C_n + C_p$)	1.6E-30 cm^6/s
Minority carrier mobility	μ_n, μ_p	Same as majority carrier mobility	Different and known
Ambipolar Diff. Coef	D_a	Decreases as mobiity	Constant
Bandgap shrinkage	ΔE_g	All over the map	Well characterized
Absorption coef.	$\alpha(\lambda)$	Not known near band edge	Well characterized
Surface rec. veloicty	s	Poorly characterized	Well characterized
Radiative rec. coef.	B	9.5E-15 cm^3/s or 2.1E-15 cm^3/s	9.5E-15 cm^3/s actual 2.1E-15 cm^3/s apparent
Specific contact res.	R_c	Poorly characterized	Well characterized
Light trapping		Not understood	Well characterized
2D and 3D effects		Not considered	Well characterized

on

History of Limit Efficiency Calculations

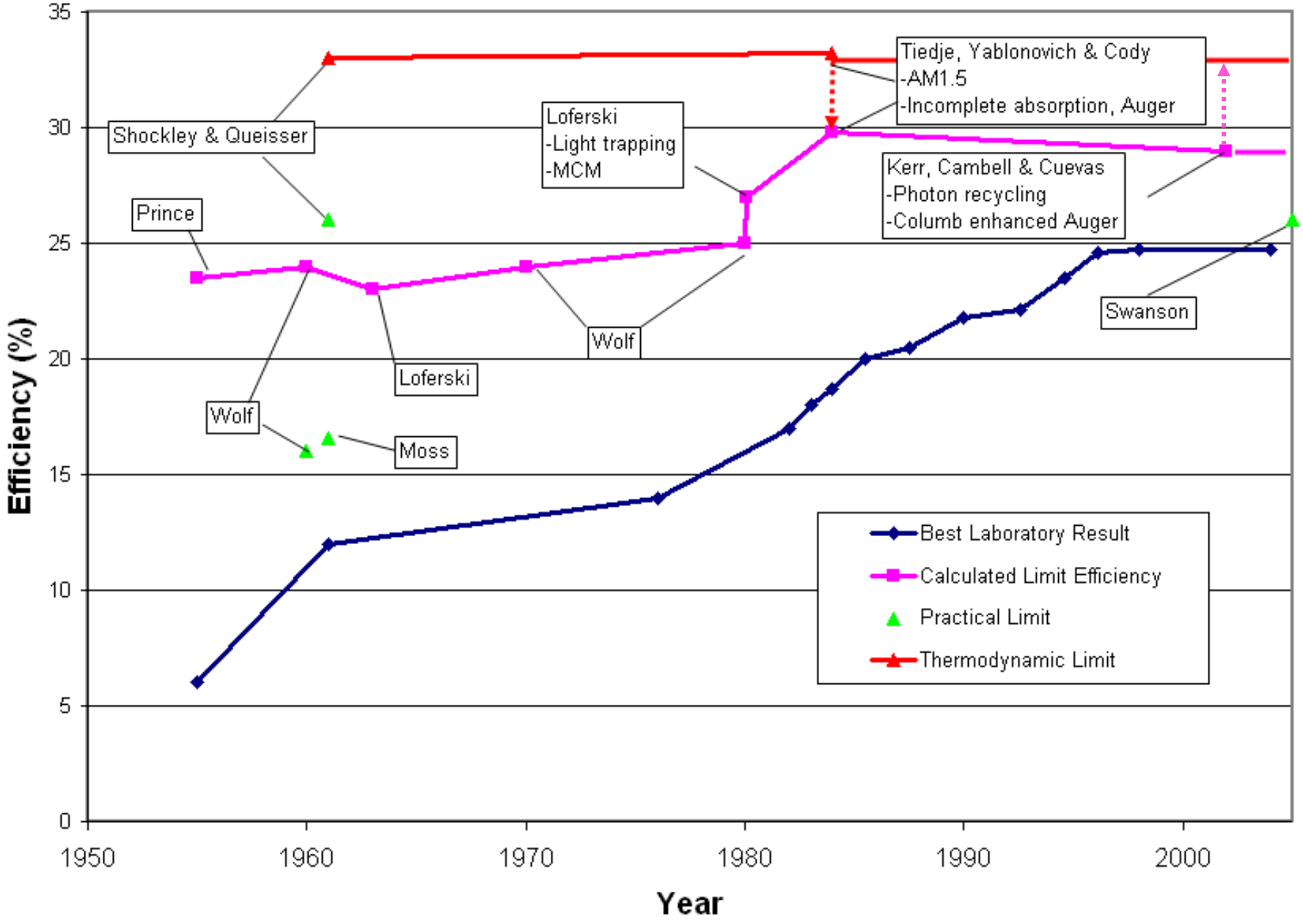

The Detail Balance Argument of Shockley and Queisser

- At room temperature, the current of blackbody with energy greater than 1.12 eV photons striking a surface is

$0.27\ fA/cm^{-2}$

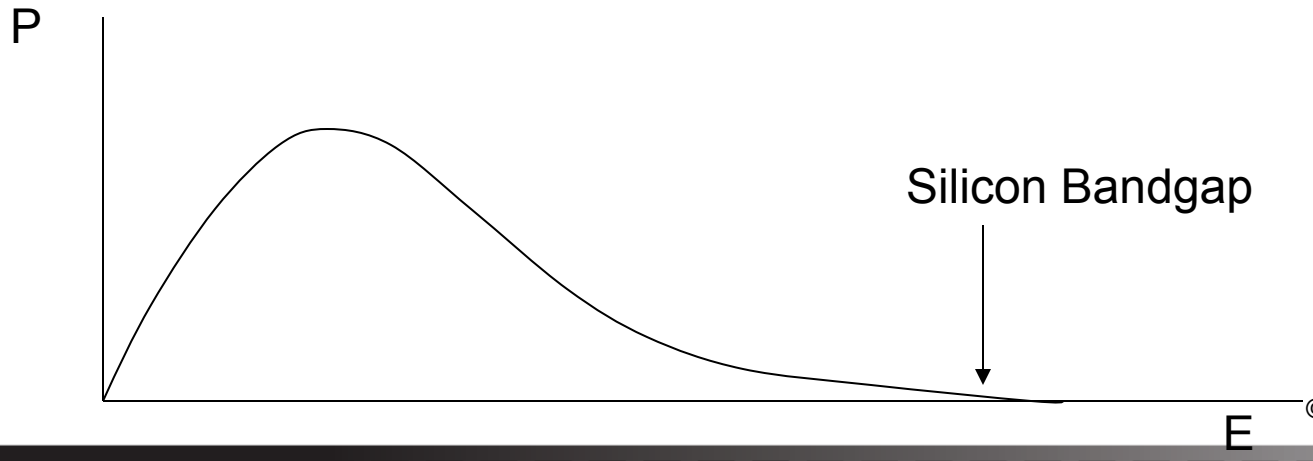

Room Temperature Blackbody Photon Spectrum

1980, Loferski adds Light-Trapping and Minority Carrier Mirrors

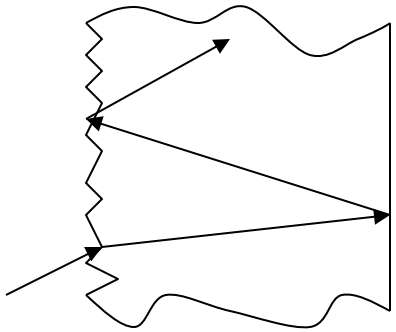

Light Trapping

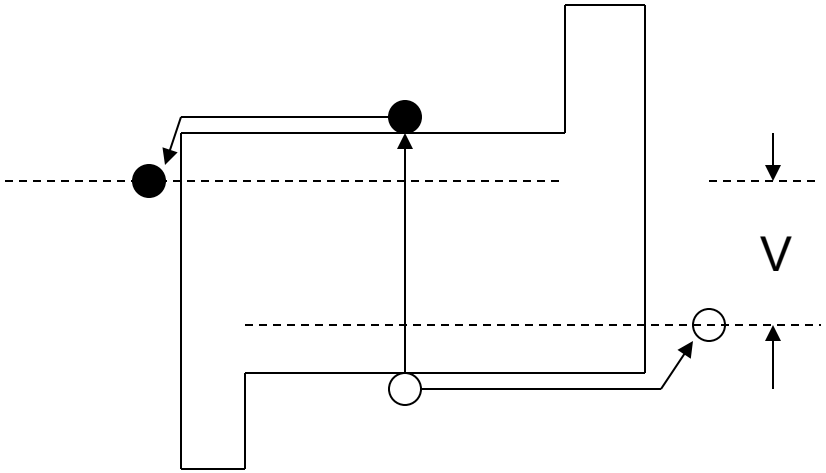

Minority Carrier Mirrors,
Or Heterojunction
Contacts (s=0)

History of Limit Efficiency Calculations

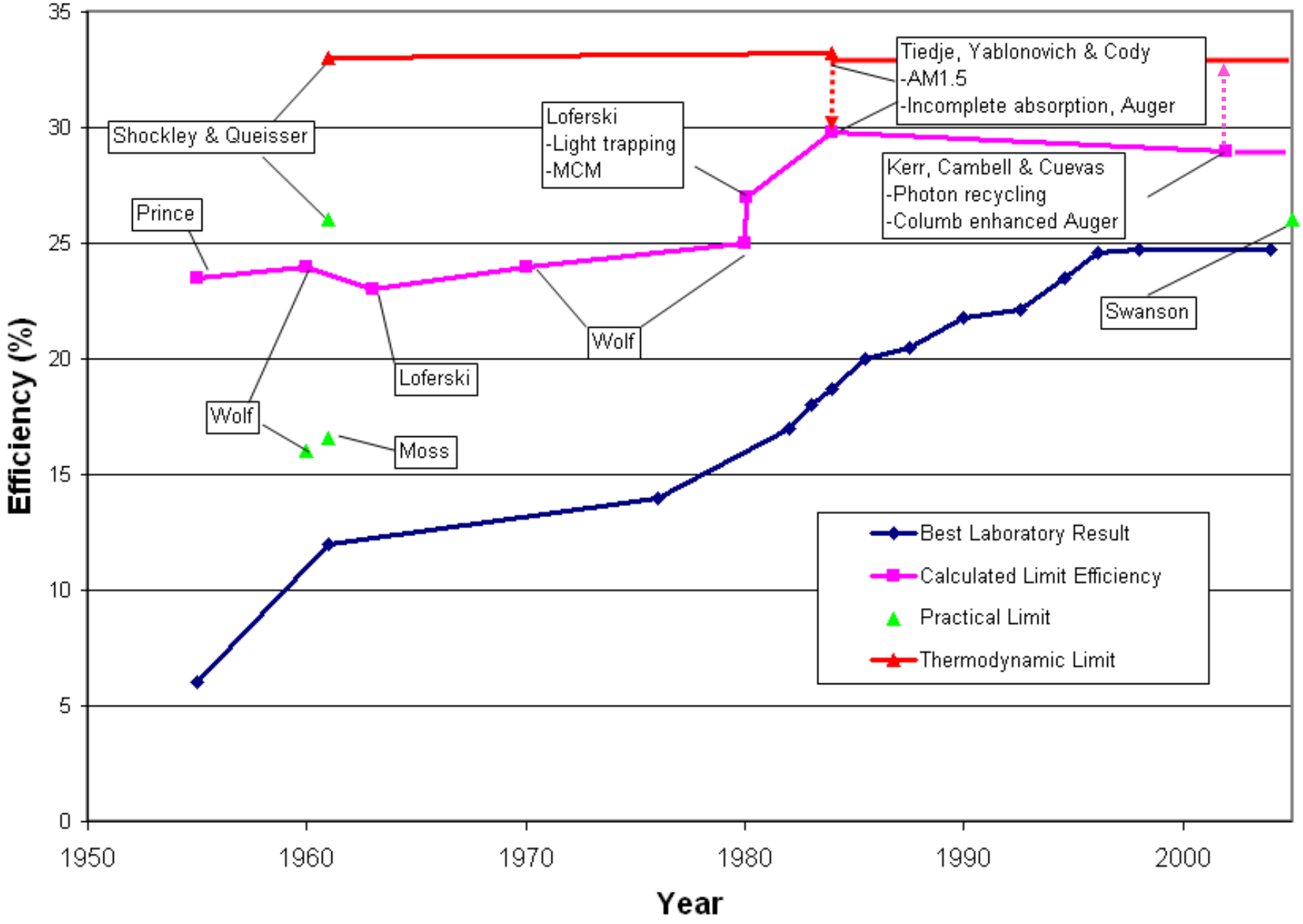

IEEE TRANSACTIONS ON ELECTRON DEVICES, VOL. ED-31, NO. 5, MAY 1984

Limiting Efficiency of Silicon Solar Cells

TOM TIEDJE, ELI YABLONOVITCH, GEORGE D. CODY, AND BONNIE G. BROOKS

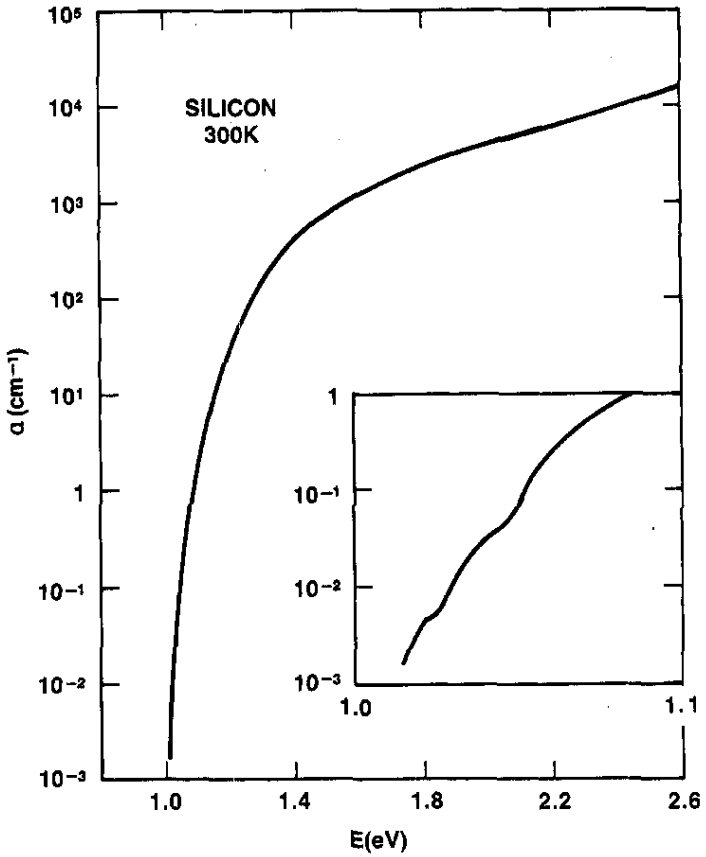

Fig. 3. Optical absorption coefficient of silicon at 300 K in the vicinity of the band edge [12].

History of Limit Efficiency Calculations

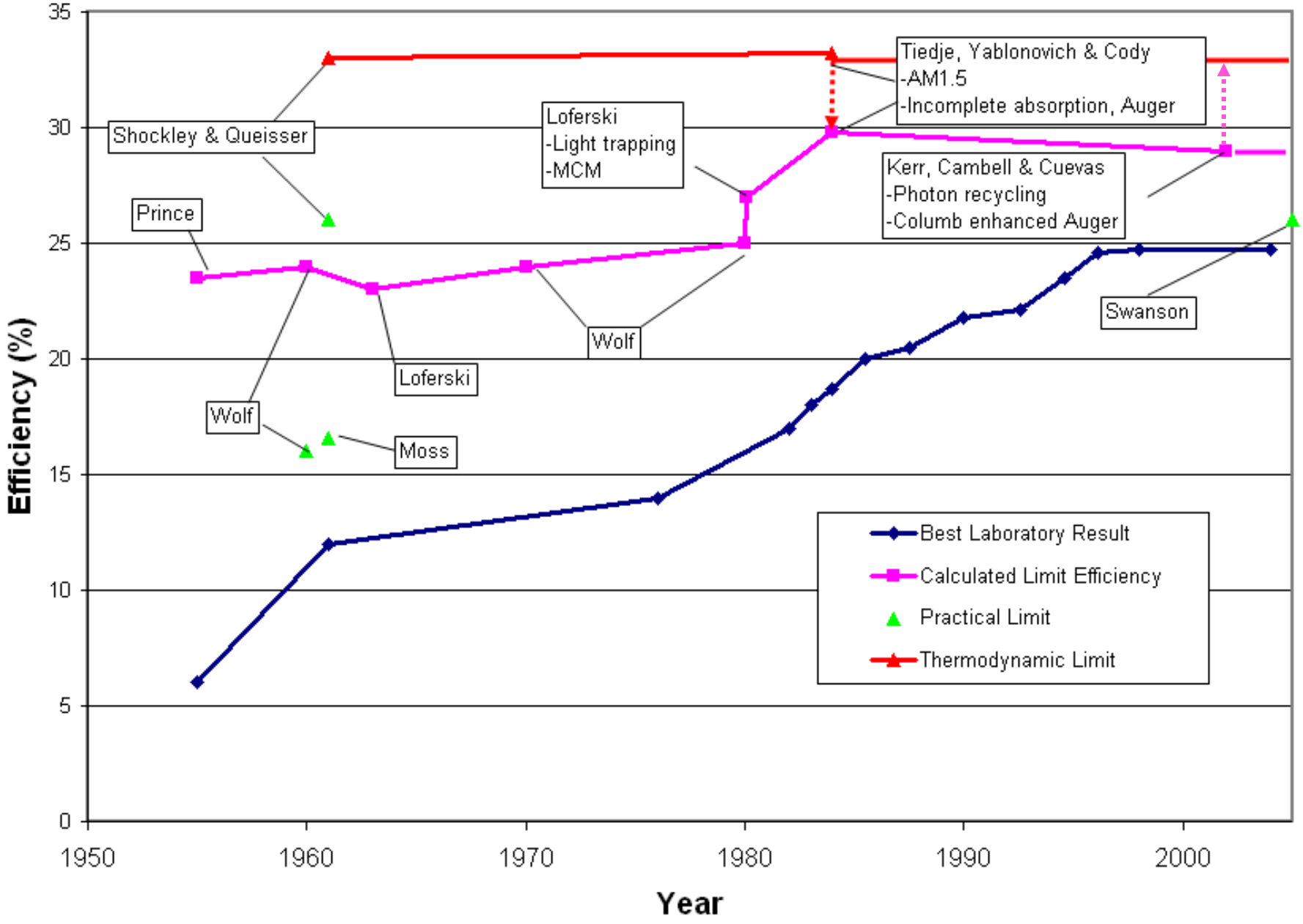

IEEE TRANSACTIONS ON ELECTRON DEVICES, VOL. ED-34, NO. 6, JUNE 1987

Recombination in Highly Injected Silicon

RONALD A. SINTON AND RICHARD M. SWANSON, MEMBER, IEEE

Abstract—Recent advances in solar cells designed to operate under high-level injection conditions have produced devices that are approaching some of the limits imposed by the fundamental band-to-band Auger recombination in silicon. A device has been optimized to study this recombination by using the fabrication technology developed for point-contact solar cells. Using both steady-state and transient measurements, the recombination rates in high-resistivity Si in the injected carrier density range of 10^{15} to 2×10^{17} carriers/cm^3 were investigated. The coefficient of the recombination, which depends on the carrier density cubed, is found to be 1.66×10^{-30} cm^6/s $\pm$ 15 percent. This result is four times higher than the ambipolar Auger coefficient commonly used in the modeling of devices that operate in this injected carrier density range and lowers the expected limit efficiencies for silicon solar cells.

Coulomb Enhanced Auger Resolves Discrepancy

LIFETIME AND EFFICIENCY LIMITS OF CRYSTALLINE SILICON SOLAR CELLS

Mark J. Kerr[1], Patrick Campbell[2] and Andres Cuevas[1]
[1]Department of Engineering, The Australian National University, Canberra ACT 0200, Australia
[2]Photovoltaics Special Research Centre, UNSW, Sydney NSW 2052, Australia

ABSTRACT

A new parameterization for Auger recombination in silicon has been determined, which accurately fits the highest available experimental lifetime data for arbitrary injection level and dopant density, for both *n*-type and *p*-type dopants. Our analysis confirms that Auger recombination is enhanced above the traditional free-particle rate at both low injection and high injection conditions. The new parameterization is used to show that Coulomb-enhanced Auger recombination imposes the most severe bound on the achievable efficiency of crystalline silicon solar cells, with a maximum limiting efficiency of 29.05% determined for a high resistivity silicon base (90μm thick). The limiting efficiency reduces for more heavily doped silicon and is lower for *n*-type silicon compared to *p*-type silicon.

PROGRESS IN PHOTOVOLTAICS: RESEARCH AND APPLICATIONS
Prog. Photovolt: Res. Appl. 2003; **11**:97–104 (DOI: 10.1002/pip.464)

Research

Limiting Efficiency of Crystalline Silicon Solar Cells Due to Coulomb-Enhanced Auger Recombination

Mark J. Kerr[1,*,†], Andres Cuevas[1] and Patrick Campbell[2]
[1]*Centre for Sustainable Energy Systems, Deptartment of Engineering, FEIT, Australian National University, Canberra ACT 0200, Australia*
[2]*Photovoltaics Special Research Centre, University of New South Wales, Sydney, NSW 2052, Australia*

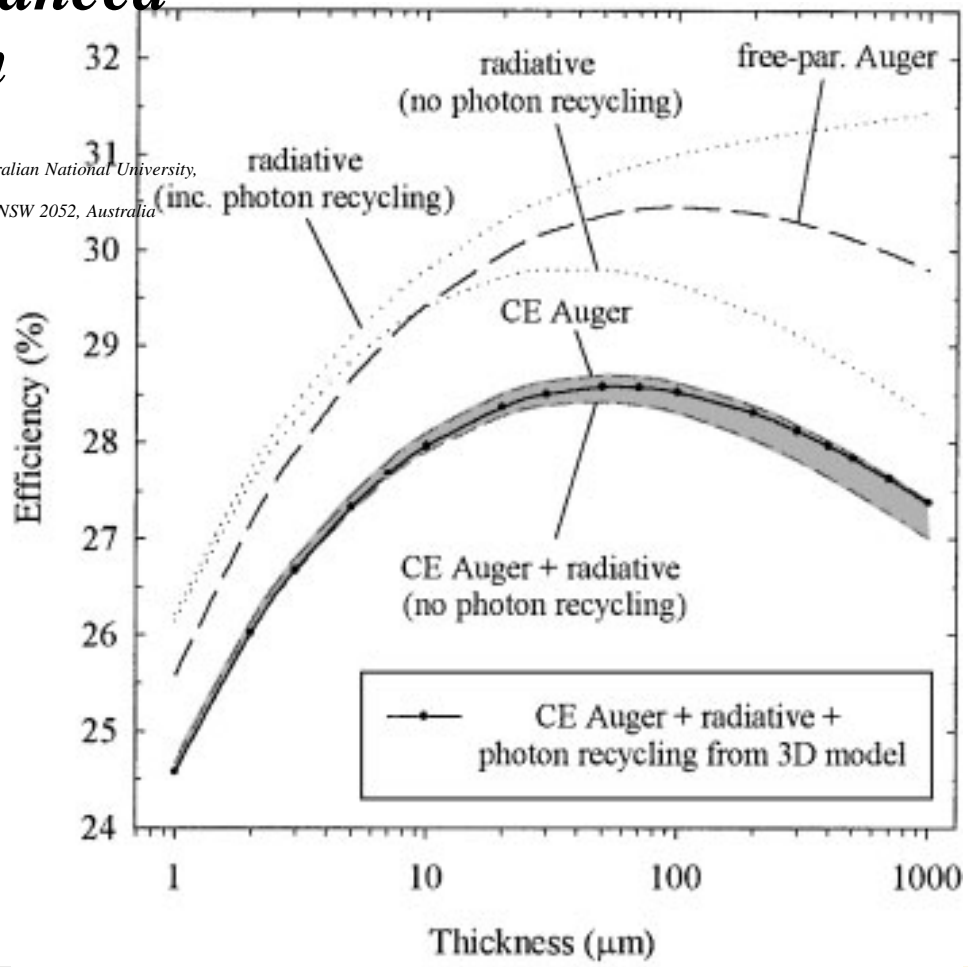

Photon Recycling Decreases the Effective Radiative Recombination

$$R_{rad} = Bpn$$

$$B_{eff} = KB$$

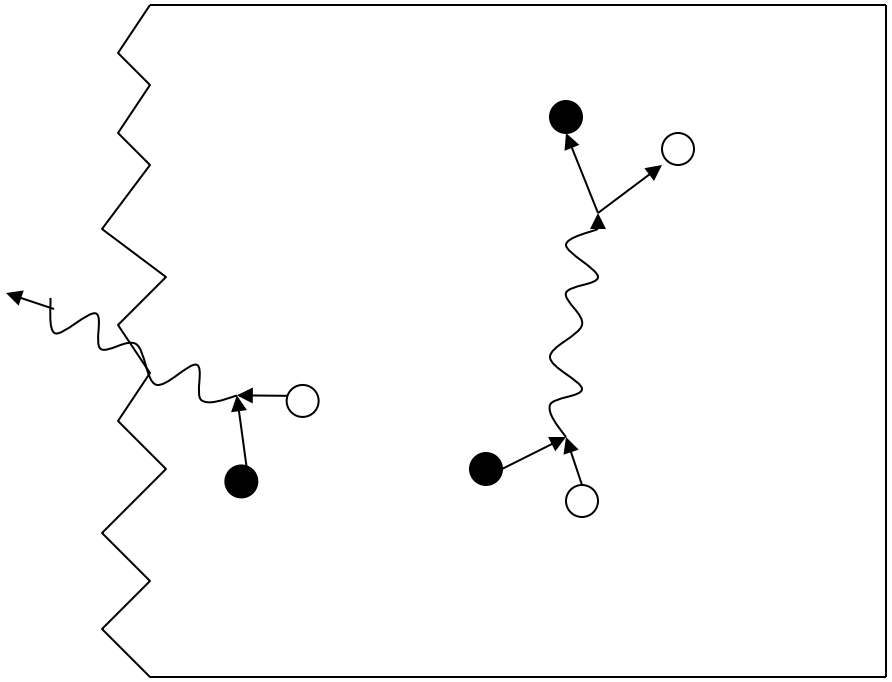

B = 9.5 X 10^{-15} cm^3/sec

But

B_{eff} = 2.1 X 10^{-15} cm^3/sec

For typical cells with good light trapping

2000-2002, Green, Kerr, Campbell, and Cuevas

History of Limit Efficiency Calculations

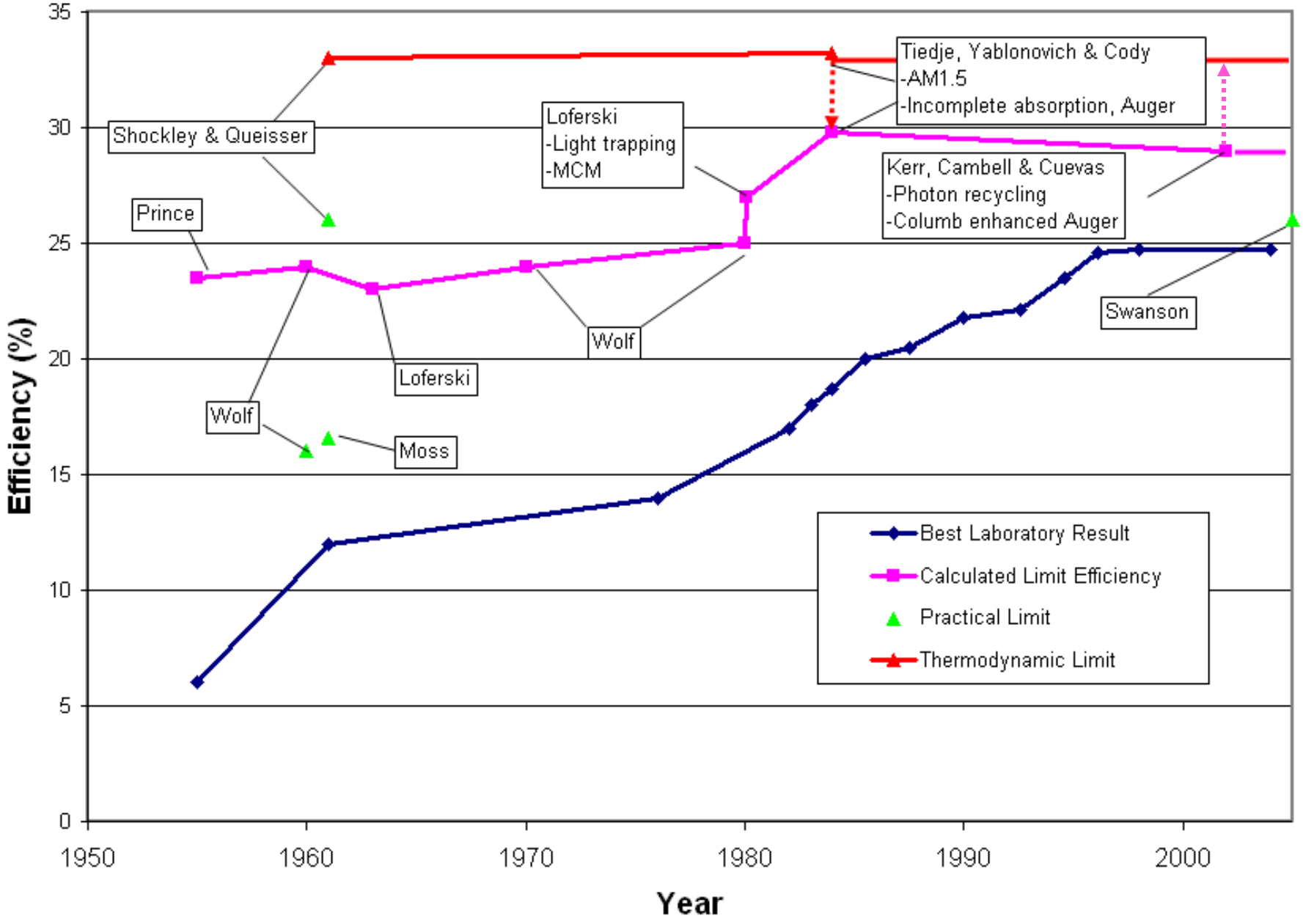

Losses Going From the Thermodynamic Limit to the Silicon Limit Cell

Step	%	
Thermodynamic limit	33.2	1.15 eV
Silicon band-gap	32.7	1.12 eV
Incomplete absorption	31.6	Thermodynamic or PC1D, $W \rightarrow \infty$
Auger recombination	29.0	
Silicon Limit	28.9	Finite mobility

MEASUREMENT OF THE EMITTER SATURATION CURRENT BY A CONTACTLESS PHOTOCONDUCTIVITY DECAY METHOD

D. E. Kane, R. M. Swanson

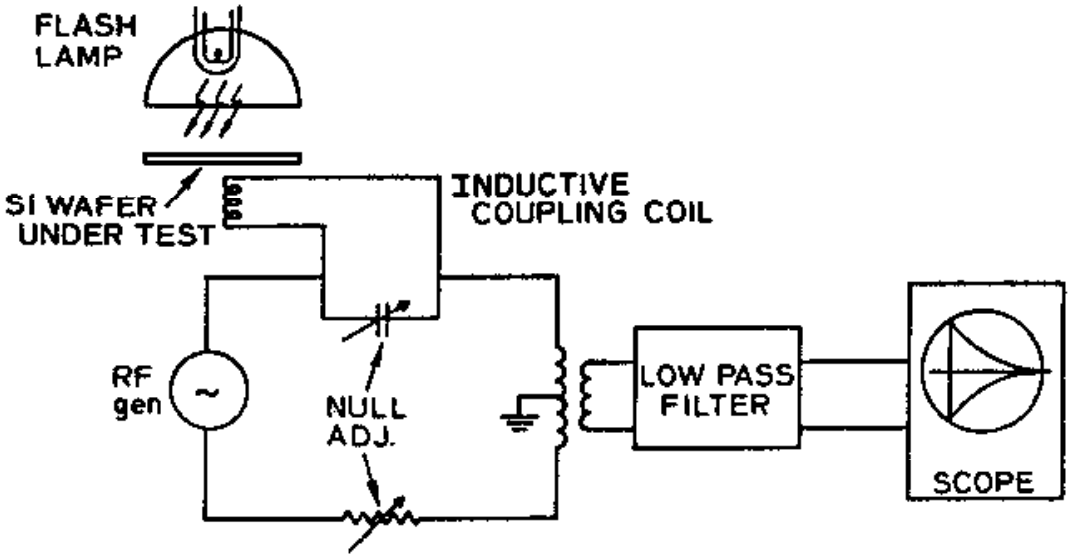

Fig. 2. - The photoconductivity measuring circuit. The steady-state conductivity is nulled out by the bridge.

Separating diffusion region recombination and bulk recombination

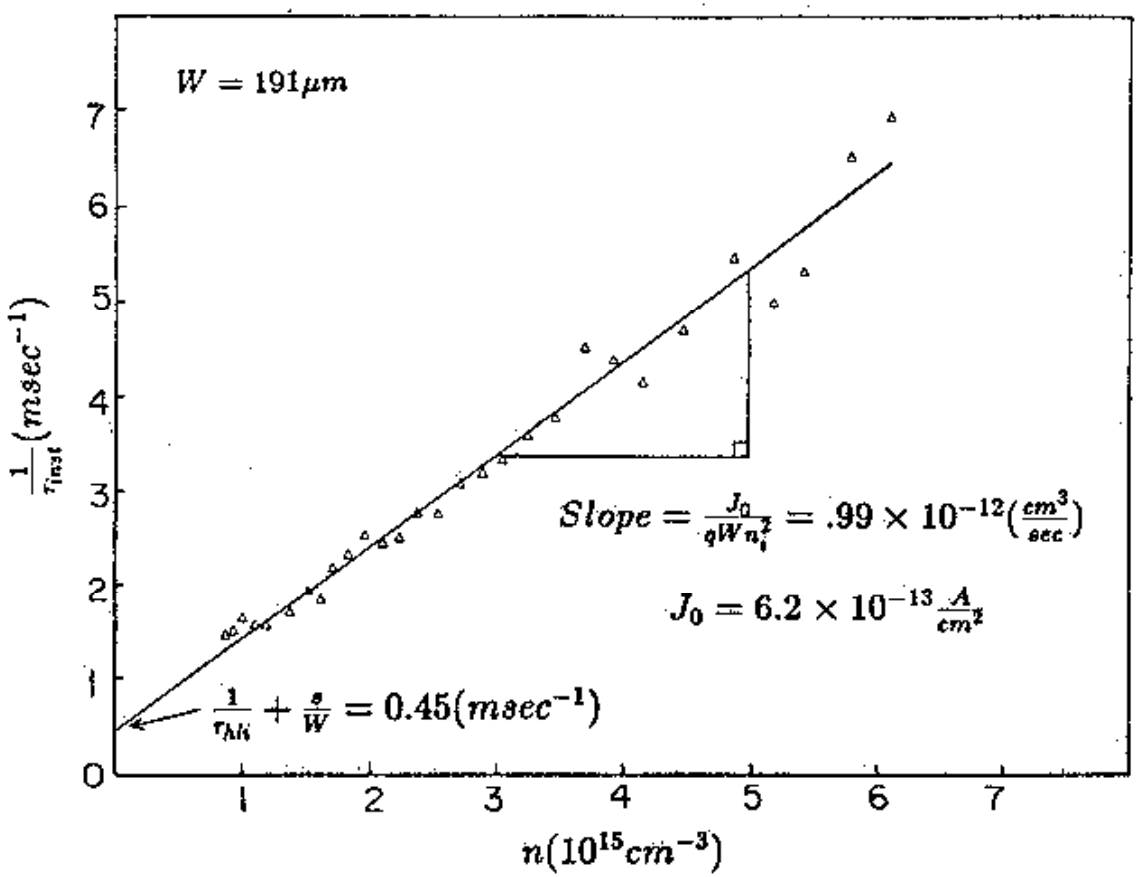

Fig. 6. - Typical experimental plot. The reciprocal decay time vs. injection level.

Measuring lifetime and J_0 is now quick and easy

Phosphorous emitters
Substrate: $N \approx 10^{13}$ cm^{-3}

$R_{sh}(\frac{\Omega}{\square})$	$x_j(\mu m)$	$N_{surf}(cm^{-3})$	$J_{0,pass}(\frac{pA}{cm^2})$	$J_{0,Al}(\frac{pA}{cm^2})$
9.0	5.8	5.0×10^{19}	0.45	0.50
57.2	3.6	1.2×10^{19}	0.10	1.10
75.3	1.8	2.0×10^{19}	0.13	1.70
370	1.2	2.5×10^{18}	0.08	1.70
890	1.3	1.0×10^{18}	0.01	7.00

Boron emitters
Substrate: $N \approx 10^{13}$ cm^{-3}

$R_{sh}(\frac{\Omega}{\square})$	$x_j(\mu m)$	$N_{surf}(cm^{-3})$	$J_{0,pass}(\frac{pA}{cm^2})$	$J_{0,Al}(\frac{pA}{cm^2})$
5.3	4.8	7.0×10^{19}	0.35	0.42
37	2.1	3.6×10^{19}	0.07	0.57
63	3.0	1.3×10^{19}	0.09	1.10
240	1.1	5.4×10^{18}	0.13	1.00
463	1.2	1.3×10^{18}	0.06	1.10

Data on surface recombination at diffused surfaces was now measureable

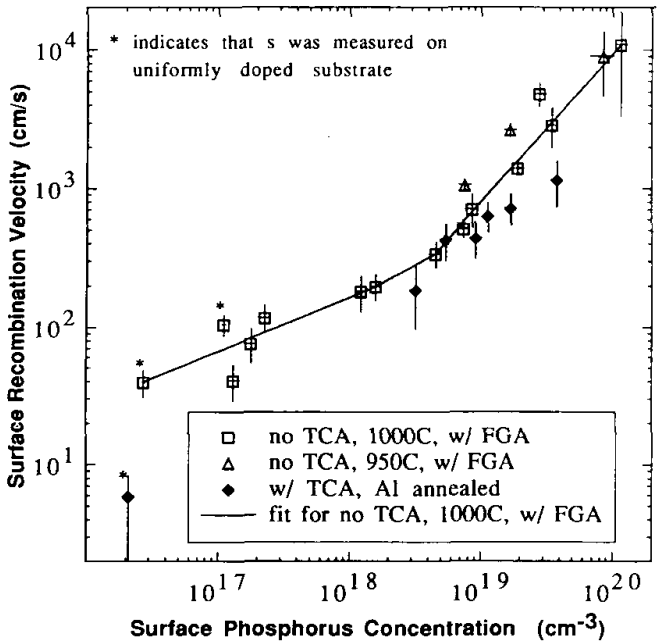

Fig. 4. Surface recombination velocity s extracted from measurements of J_0 on untextured, oxide-passivated phosphorus diffusions, using a numerical emitter model. The value of s for the starred points was measured using several thicknesses of wafers with uniform phosphorus doping.

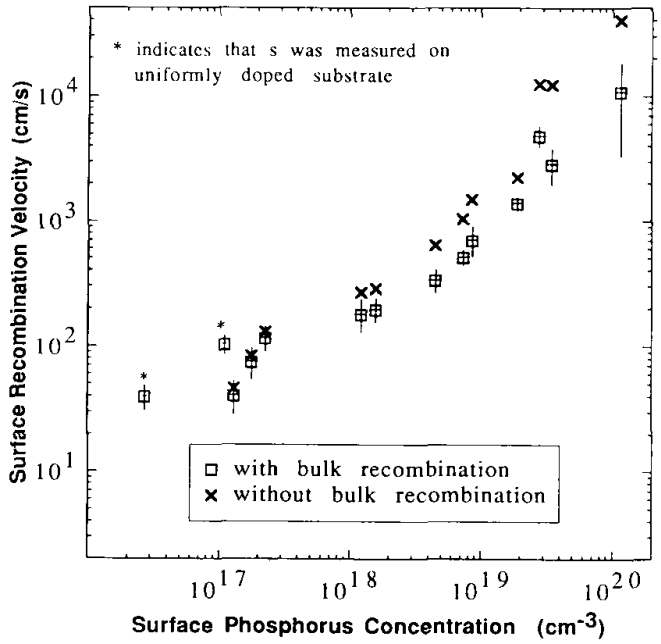

Fig. 5. Surface recombination velocity s extracted for both the standard case, in which the bulk recombination in the passivated emitter is accounted for, and the case in which there is no bulk recombination. The latter case gives an upper limit for s.

MEASURING AND MODELING MINORITY CARRIER TRANSPORT IN HEAVILY DOPED SILICON

J. DEL ALAMO, S. SWIRHUN and R. M. SWANSON
Stanford Electronics Laboratories, Stanford University, Stanford, CA 94305, U.S.A.

Reported band-gap shrinkage as all over the map

$$J_p = -qn_{i0}^2 \frac{D_p}{N_{D\,\mathrm{eff}}} \frac{\mathrm{d}u}{\mathrm{d}x}$$

$$\frac{\mathrm{d}J_p}{\mathrm{d}x} = -qn_{i0}^2 \frac{D_p}{N_{D\,\mathrm{eff}}} \frac{u}{L_p^2}.$$

$$u = \frac{p}{p_0} - 1 = \mathrm{e}^{q(\phi_p - \phi_n)/kT} - 1$$

$$p_0 N_{D\,\mathrm{eff}} = n_{i0}^2$$

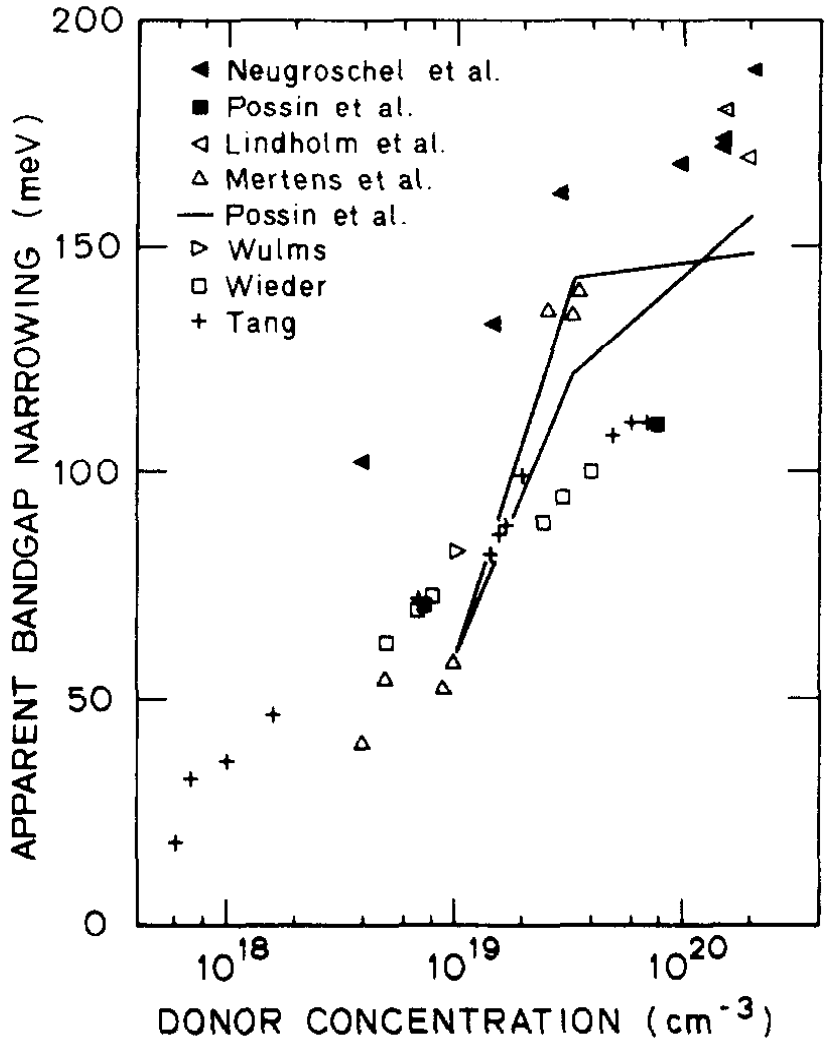

on

Adjusting for D_p differences resolved issue

$$J_p = -qn_{i0}^2 \frac{D_p}{N_{D\,\mathrm{eff}}} \frac{\mathrm{d}u}{\mathrm{d}x}$$

$$\frac{\mathrm{d}J_p}{\mathrm{d}x} = -qn_{i0}^2 \frac{D_p}{N_{D\,\mathrm{eff}}} \frac{u}{L_p^2}.$$

$$u = \frac{p}{p_0} - 1 = \mathrm{e}^{q(\phi_p - \phi_n)/kT} - 1$$

$$p_0 N_{D\,\mathrm{eff}} = n_{i0}^2$$

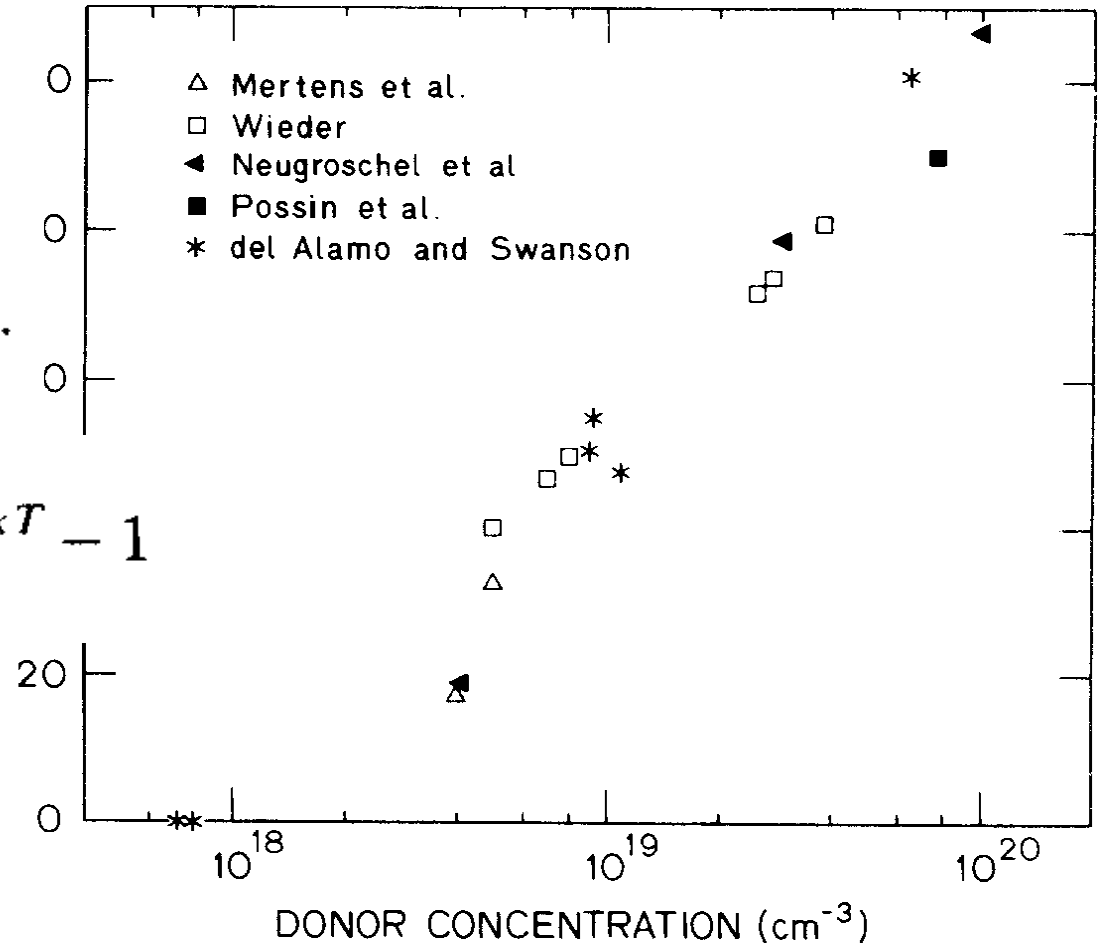

Design Criteria for Si Point-Contact Concentrator Solar Cells

RONALD A. SINTON AND RICHARD M. SWANSON, MEMBER, IEEE

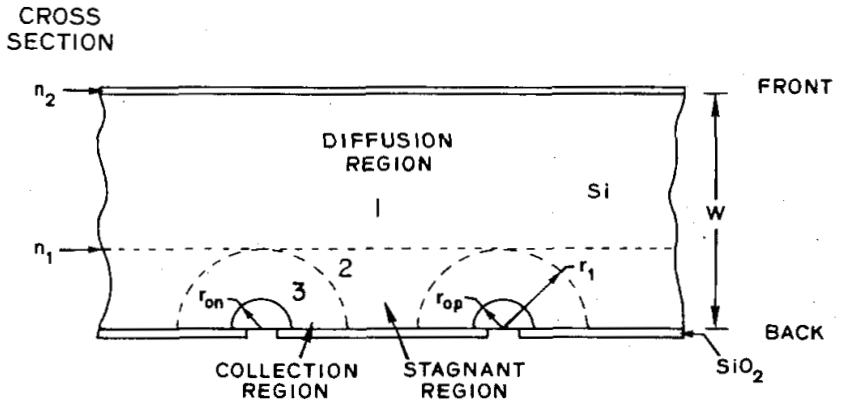

Fig. 1. A cross section of a point-contact solar cell showing the three regions considered in the modeling.

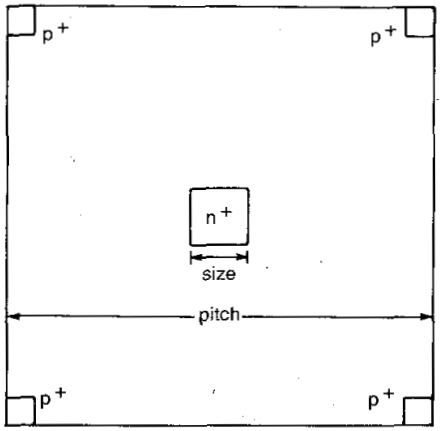

Fig. 2. A unit cell which defines the geometry of the diffusions on the backside of the wafer.

Predictive Modeling of the PCC Was Now a Reality

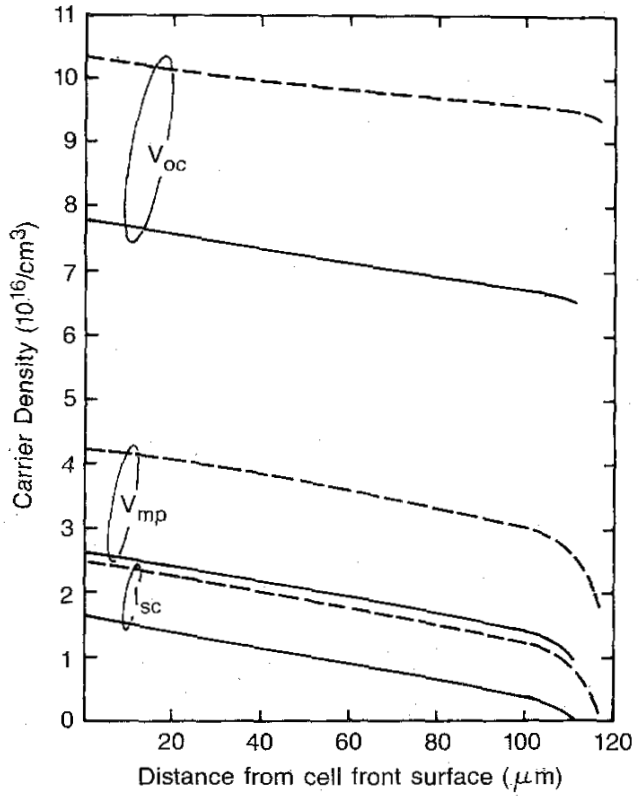

Fig. 5. The modeled carrier density profile n as a function of position from front to back in the solar cell along a line into a p^+ contact. Curves are shown for cells with 8-μm^2 diffusions (dashed curve) and 20 μm diffusions (solid curve), both on a 50-μm pitch. 10 W/cm^2, 300 K.

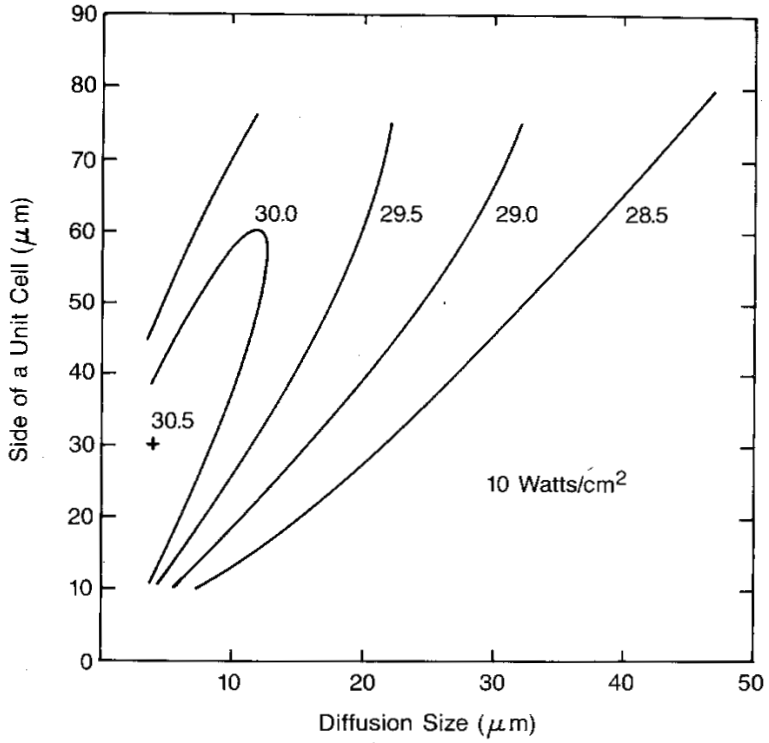

Fig. 7. Modeled contours of constant efficiency as a function of diffusion spacing (pitch) and square size. The cell is 50 μm thick and the incident intensity is 10 W/cm^2, 300 K.

Physics of Semiconductor Devices

SECOND EDITION

S. M. Sze

Bell Laboratories, Incorporated
Murray Hill, New Jersey

Properties	Ge	Si	GaAs
Atoms/cm^3	4.42×10^{22}	5.0×10^{22}	4.42×10^{22}
Atomic weight	72.60	28.09	144.63
Breakdown field(V/cm)	$\sim 10^5$	$\sim 3 \times 10^5$	$\sim 4 \times 10^5$
Crystal structure	Diamond	Diamond	Zincblende
Density (g/cm^3)	5.3267	2.328	5.32
Dielectric constant	16.0	11.9	13.1
Effective density of states in conduction band, N_C (cm^{-3})	1.04×10^{19}	2.8×10^{19}	4.7×10^{17}
Effective density of states in valence band, N_V (cm^{-3})	6.0×10^{18}	1.04×10^{19}	7.0×10^{18}
Effective Mass, m^*/m_0			
Electrons	$m_l^* = 1.64$ $m_t^* = 0.082$	$m_l^* = 0.98$ $m_t^* = 0.19$	0.067
Holes	$m_{lh}^* = 0.044$ $m_{hh}^* = 0.28$	$m_{lh}^* = 0.16$ $m_{hh}^* = 0.49$	$m_{lh}^* = 0.082$ $m_{lh}^* = 0.45$
Electron affinity, χ(V)	4.0	4.05	4.07
Energy gap (eV) at 300 K	0.66	1.12	1.424
Intrinsic carrier concentration (cm^{-3})	2.4×10^{13}	1.45×10^{10}	1.79×10^6
Intrinsic Debye length (μm)	0.68	24	2250
Intrinsic resistivity (Ω-cm)	47	2.3×10^5	10^8
Lattice constant (Å)	5.64613	5.43095	5.6533

The Missing 19 mV found!

Improved value for the silicon intrinsic carrier concentration at 300 K

A. B. Sproul, M. A. Green, and J. Zhao
Joint Microelectronics Research Centre, University of New South Wales, Kensington 2033, Australia

(Received 19 February 1990; accepted for publication 7 May 1990)

A recent review suggests that the commonly cited value of 1.45×10^{10} cm^{-3} for the silicon intrinsic carrier concentration at 300 K is inconsistent with the best experimental and theoretical results. An alternative value of 1.08×10^{10} cm^{-3} was suggested. A new experimental measurement of 1.01×10^{10} cm^{-3} is reported with an estimated one standard deviation uncertainty of only 3%. This appears to be the most accurate experimental determination of this parameter at any temperature.

Appl. Phys. Lett. **57** (3), 16 July 1990

Importance of an Oxide at the Back Surface

SILICON SOLAR CELLS
Advanced Principles
& Practice

Martin A. Green

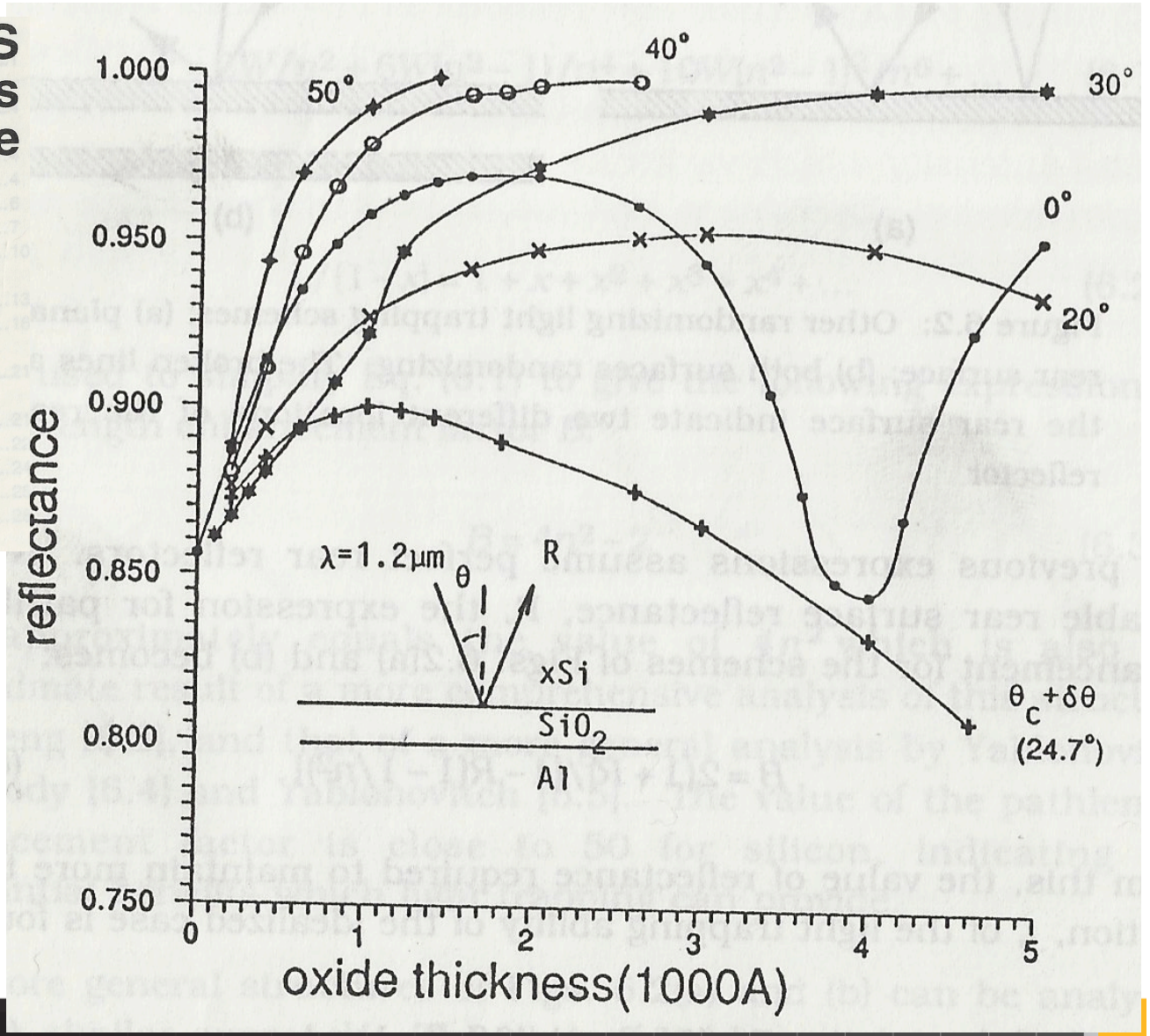

Efficiency Loss Waterfall

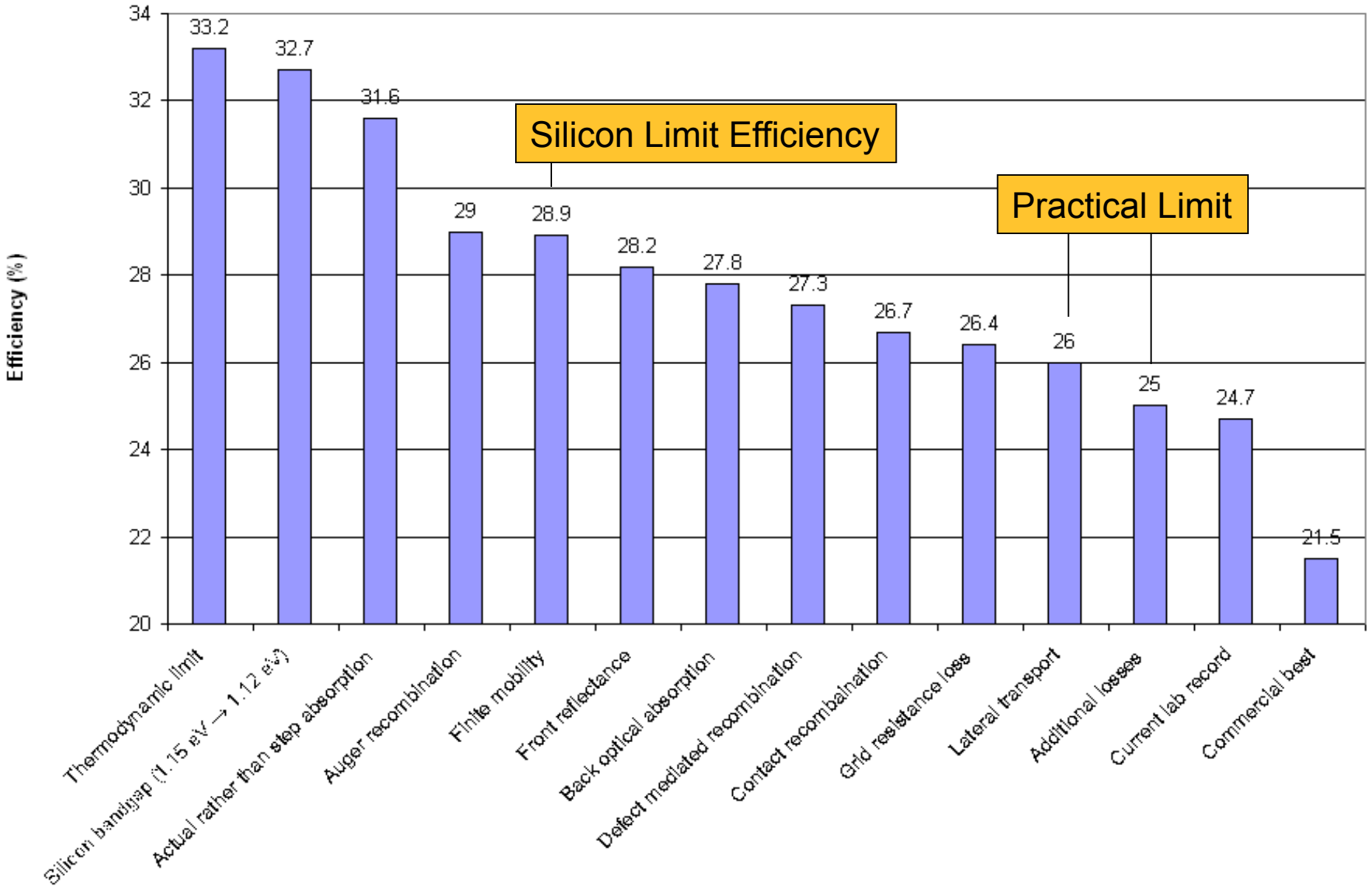

Efficiency Loss Waterfall